

Solution and Solid State Multinuclear NMR Investigation of the Structure of $\{(\text{BuSn})_{12}\text{O}_{14}(\text{OH})_6\}(\text{O}_2\text{PPh}_2)_2$

François Ribot* and Clément Sanchez

Université P. et M. Curie, Chimie de la Matière Condensée (CNRS UMR 7574), F-75252 Paris, France

Rudolph Willem, José C. Martins, and Monique Biesemans

Free University of Brussels (VUB), High-Resolution NMR Centre, Pleinlaan 2, B-1050 Brussel, Belgium

Received September 18, 1997

$\{(\text{BuSn})_{12}\text{O}_{14}(\text{OH})_6\}(\text{O}_2\text{PPh}_2)_2$ has been prepared from $\{(\text{BuSn})_{12}\text{O}_{14}(\text{OH})_6\}(\text{OH})_2$ and diphenylphosphinic acid. Its full characterization by solution 1D (^1H , ^{13}C , ^{119}Sn , and ^{31}P) and 2D gradient-assisted (^1H – ^{119}Sn HMQC, ^1H – ^{13}C HMQC, ^1H ROESY, and ^{31}P – ^1H HOESY) NMR is reported and shows that in CD_2Cl_2 or $\text{CD}_2\text{Cl}_2/\text{DMSO}-d_6$ (1/1) the charge compensating diphenylphosphinate anions remain close to the “cage-poles” of the macrocations. A model for the geometry of the interaction is proposed. ^{119}Sn and ^{31}P MAS NMR characterization of the title compound is also reported.

Introduction

The dicationic, closo-type cluster $\{(\text{BuSn})_{12}\text{O}_{14}(\text{OH})_6\}^{2+}$ exists in combination with several anions^{1–4} and has been isolated in the crystalline state, both as $\{(\text{BuSn})_{12}\text{O}_{14}(\text{OH})_6\}\text{Cl}_2 \cdot 2\text{H}_2\text{O}$ ¹ and as $\{(\text{BuSn})_{12}\text{O}_{14}(\text{OH})_6\}(\text{OH})_2 \cdot (\text{PrOH})_4$.² The structure of the macrocation can be viewed as a centrosymmetric, almost spherical, cage composed of twelve tin atoms linked by $\mu_3\text{-O}$ bridges (see Figure 1). Six five-coordinate tin atoms are located at the “cage equator” and exhibit a distorted square pyramidal geometry. Three six-coordinate tin atoms are found at each of the two “cage poles” and exhibit a distorted octahedral geometry involving also $\mu_2\text{-OH}$ bridges.^{1,2} In the crystalline state, the two anions, compensating the 2-fold positive charge of the macrocation, are symmetrically located at the “cage poles” and are involved in a complex network of hydrogen bonds including likewise solvent molecules.^{1,2} The exact symmetry of the $\{(\text{BuSn})_{12}\text{O}_{14}(\text{OH})_6\}^{2+}$ core, as determined from single-crystal X-ray diffraction,^{1,2} is quite low and consists only of an inversion center. Solid state ^{119}Sn NMR experiments, performed on $\{(\text{BuSn})_{12}\text{O}_{14}(\text{OH})_6\}(\text{OH})_2 \cdot (\text{PrOH})_4$ ² and $\{(\text{BuSn})_{12}\text{O}_{14}(\text{OH})_6\}(\text{O}_2\text{CCH}_3)_2$ ³, indicate a higher apparent symmetry (C_{2h}), including a mirror plane which slices the Sn–O–Sn framework perpendicularly to the “cage equator” (along a meridian). Actually, this mirror plane is a pseudo-element of symmetry in the X-ray diffraction structure if the β , γ , and δ carbon atoms of the butyl chains are omitted.² $\{(\text{BuSn})_{12}\text{O}_{14}(\text{OH})_6\}\text{X}_2$ ($\text{X} = \text{Cl}^-$, OH^- , CH_3CO_2^- , $p\text{-CH}_3\text{C}_6\text{H}_4\text{SO}_3^-$)^{1–4} exhibits an even higher symmetry in solution. Solution ^{119}Sn NMR shows only

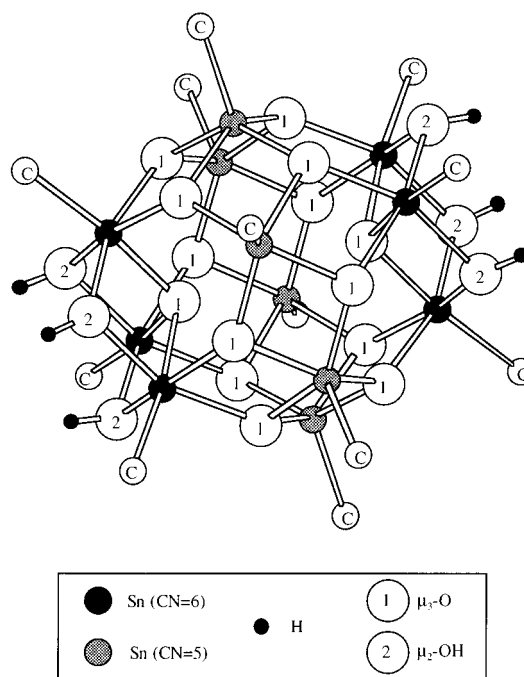


Figure 1. Schematic view of the closo-type cluster $\{(\text{BuSn})_{12}\text{O}_{14}(\text{OH})_6\}^{2+}$. Only the α -carbon of each butyl chain is shown for clarity.

two ^{119}Sn chemical shifts, around -280 and -450 ppm, which are related to five- and six-coordinate tin atoms, respectively.^{1–4} These results are in agreement with a 3-fold symmetry (D_{3d}), on the observational NMR time scale, the C_3 axis passing through the two $\mu_3\text{-O}$ atoms bridging the three six-coordinate tin atoms at each “cage pole”. This 3-fold symmetry is still observed by solution ^{119}Sn NMR, even when the anions have a lower symmetry (i.e. CH_3CO_2^-).³ This can be interpreted by the ionic dissociation of the original entities, $\{(\text{BuSn})_{12}\text{O}_{14}(\text{OH})_6\}^{2+} + 2\text{X}^-$. Yet the clear influence of the anions on the ^{119}Sn chemical shifts (of mainly the six-coordinate tin atoms),

- (1) Dakternieks, D.; Zhu, H.; Tiekink, E. R. T.; Colton, R. *J. Organomet. Chem.* **1994**, *476*, 33.
- (2) Banse, F.; Ribot, F.; Tolédano, P.; Maquet, J.; Sanchez, C. *Inorg. Chem.* **1995**, *34*, 6371.
- (3) Ribot, F.; Banse, F.; Diter, F.; Sanchez, C. *New J. Chem.* **1995**, *19*, 1145.
- (4) Ribot, F.; Eychenne-Baron, C.; Banse, F.; Sanchez, C. *Better Ceramics through Chemistry VII: Organic/Inorganic Hybrid Materials*; Coltrain, B. K., Sanchez, C., Schaefer, D. W., Wilkes, G. L., Eds.; Materials Research Society: Pittsburgh, PA, 1996; p 43.

the good agreement between solution and solid state (isotropic) ^{119}Sn chemical shifts, and, finally, the fairly low dielectric constants (~ 5) of the solvents used for NMR greatly favor the presence of the anions in the vicinity of the "cage poles" in solution.^{2,3} Therefore, the exact behavior of $\{(\text{BuSn})_{12}\text{O}_{14}(\text{OH})_6\}\text{X}_2$ in solution remains to be clarified.

Actually, the interactions taking place between the macrocation and its charge compensating anions are relevant to material science as they have allowed us to prepare hybrid organic–inorganic polymers⁵ by assembling $\{(\text{BuSn})_{12}\text{O}_{14}(\text{OH})_6\}^{2+}$ clusters. These perfectly defined nanobuilding blocks can either be turned into alternated hybrid copolymers by reacting them with telechelic dianions^{3,4} or be first functionalized with peculiar anions and then assembled by taking advantage of the reactivity of these anions (i.e., methacrylate and radical polymerization).⁶ Therefore, a good knowledge of the macrocation–anion interaction should allow a better understanding of the inorganic–organic interface in these hybrid copolymers.

The purpose of the present paper is fivefold. First it is shown that upon reaction of $\{(\text{BuSn})_{12}\text{O}_{14}(\text{OH})_6\}(\text{OH})_2$ with 2 equiv of diphenylphosphinic acid, the cluster is preserved, since a compound obeying the formula $\{(\text{BuSn})_{12}\text{O}_{14}(\text{OH})_6\}(\text{O}_2\text{PPh}_2)_2$ is obtained. Second, as no crystals could be obtained so far, NMR investigations, particularly in solution, become a valuable alternative for the structural characterization of such systems. More specifically, this investigation aimed at gaining insight into the binding mode of the anions to the cluster in solution, taking advantage of the NMR response of the ^{31}P nucleus contained in the anions.

This paper presents the full characterization of $\{(\text{BuSn})_{12}\text{O}_{14}(\text{OH})_6\}(\text{O}_2\text{PPh}_2)_2$ in solution by multinuclear NMR. Two-dimensional, gradient-assisted, ^1H – ^{119}Sn and ^1H – ^{13}C HMQC spectroscopy enables full, tin atom specific, assignment of all the ^1H and ^{13}C resonances, while ^{31}P – ^1H heteronuclear NOESY experiments (HOESY), combined with homonuclear ^1H ROESY experiments, shed some light onto the location of the anions with respect to the cluster. Solid state ^{119}Sn and ^{31}P MAS NMR data are also reported.

Experimental Section

Synthesis. Crystalline $\{(\text{BuSn})_{12}\text{O}_{14}(\text{OH})_6\}(\text{OH})_2 \cdot (\text{PrOH})_4$ was prepared by hydrolysis of $\text{BuSn}(\text{O}^i\text{Pr})_3$ as previously described.² The 2-propanol solvate molecules were then removed by vacuum drying ($P \approx 10^{-2}$ mmHg and $T \approx 50$ °C) to yield amorphous $\{(\text{BuSn})_{12}\text{O}_{14}(\text{OH})_6\}(\text{OH})_2$. A 2.47 g (1.0 mmol) amount of $\{(\text{BuSn})_{12}\text{O}_{14}(\text{OH})_6\}(\text{OH})_2$ was dissolved in 46.9 g of THF, resulting in a clear 5 wt% solution of the dihydroxyl cluster. A 0.436 mg (2.0 mmol) amount of diphenylphosphinic acid, $\text{Ph}_2\text{PO}_2\text{H}$ (Aldrich), was added under magnetic stirring. The solid diphenylphosphinic acid disappeared within a few seconds. The clear THF solution was stirred for a further 10–15 min. Subsequently, the THF was removed under reduced pressure to yield a white powder that was finally dried under vacuum ($P \approx 10^{-2}$ mmHg and room temperature); 2.87 g of solid was recovered. This compound corresponds to $\{(\text{BuSn})_{12}\text{O}_{14}(\text{OH})_6\}(\text{O}_2\text{PPh}_2)_2$. Anal. Found: Sn, 49.3; C, 30.0; H, 4.9; P, 2.2. Calcd: Sn, 49.63; C, 30.13; H, 4.71; P, 2.16. Unlike its precursor, $\{(\text{BuSn})_{12}\text{O}_{14}(\text{OH})_6\}(\text{OH})_2$, $\{(\text{BuSn})_{12}\text{O}_{14}(\text{OH})_6\}(\text{O}_2\text{PPh}_2)_2$ is easily soluble in C_6H_6 , CH_2Cl_2 , and CHCl_3 .

$\{(\text{BuSn})_{12}\text{O}_{14}(\text{OH})_6\}\text{Cl}_2 \cdot 2\text{H}_2\text{O}$ was prepared from BuSnCl_3 (Strem chemicals) as described elsewhere.¹ Several recrystallizations, in acetone, were performed.

Solution NMR Experiments. The samples were prepared by dissolving ca. 50 mg of $\{(\text{BuSn})_{12}\text{O}_{14}(\text{OH})_6\}(\text{O}_2\text{PPh}_2)_2$ in 500 μL of CD_2Cl_2 or of a 1/1 mixture of $\text{CD}_2\text{Cl}_2/\text{DMSO}-d_6$. All spectra were recorded at 303 K, unless otherwise indicated, on a Bruker AMX500 spectrometer interfaced with an X32 computer and operating at 500.13, 125.77, 202.46, and 186.50 MHz for ^1H , ^{13}C , ^{31}P , and ^{119}Sn nuclei, respectively. Chemical shifts were referenced to the residual solvent peak (CD_2Cl_2) and converted to the standard Me_4Si scale by adding 5.32 and 53.8 ppm for ^1H and ^{13}C nuclei, respectively. For the ^{119}Sn and ^{31}P chemical shifts, $\Xi = 37.290\,665$ MHz and $\Xi = 40.480\,747$ MHz were used, respectively.⁷

One-dimensional ^{13}C , ^{31}P , and ^{119}Sn BB proton-decoupled spectra were recorded using standard pulse sequences and delays from the Bruker program library, as were also the 2D homonuclear (NOESY and ROESY)⁸ and the heteronuclear Overhauser correlation spectra (HOESY).⁹

The proton-detected 2D ^1H – ^{119}Sn HMQC correlation spectra were acquired without ^{119}Sn decoupling using the pulse sequences of the Bruker library¹⁰ adapted to include gradient pulses,¹¹ as proposed and illustrated recently.¹² Proton-detected ^1H – ^{13}C HMQC spectra¹⁰ with ^{13}C decoupling were likewise acquired using the gradient-adapted pulse sequences mentioned above.

Routine ^{119}Sn NMR experiments (determination of the products of the reaction of $\{(\text{BuSn})_{12}\text{O}_{14}(\text{OH})_6\}(\text{OH})_2$ with more than 2 equiv of $\text{Ph}_2\text{PO}_2\text{H}$, or of $\{(\text{BuSn})_{12}\text{O}_{14}(\text{OH})_6\}\text{Cl}_2$ with 2 equiv of $\text{Ph}_2\text{PO}_2\text{H}$) were performed on a Bruker AC300 spectrometer (111.92 MHz for ^{119}Sn), with ^1H composite pulse decoupling. In that case, ^{119}Sn chemical shift were referenced against external Me_4Sn .

Solid-State NMR Experiments. The ^{119}Sn and ^{31}P MAS (magic angle spinning) NMR experiments were performed on a Bruker MSL300 spectrometer (111.92 and 121.49 MHz for ^{119}Sn and ^{31}P , respectively) equipped with a 4 mm high-speed locked Bruker probe. For ^{119}Sn , the standard QUADCYCL pulse sequence, from the Bruker program library, was used. The spectral width was 200 000 Hz (≈ 1800 ppm), and pulse angles and recycling delays were about 30° (1.5 μs) and 10 s, respectively. Typically 1000–5000 transients were necessary to achieve reasonable signal-to-noise ratios. ^{119}Sn chemical shifts are quoted relative to Me_4Sn , using solid tetracyclohexyltin ($\delta_{\text{iso}} = -97.35$ ppm) as a secondary external reference.¹³ For ^{31}P , QUADCYCL or HPDEC (high-power ^1H decoupling during acquisition, from the Bruker program library) pulse sequences were used at high (10 000 Hz) or low (3000 Hz) spinning speeds, respectively. ^1H decoupling at low spinning speed was necessary to remove the ^1H – ^{31}P dipolar interaction which is not fully averaged to zero and dramatically broadens the resonances. The spectral width was 60 000 Hz (≈ 500 ppm). Pulse angles and recycling delays were about 30° (1.0 μs) and 10 s, respectively. Depending on the spinning rate, 32–400 transients were

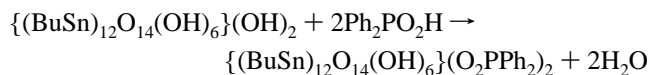
- (5) (a) Schmidt, H.; Seiferling, B. *Mater. Res. Soc. Symp. Proc.* **1986**, 73, 739. (b) Novak, B. M. *Adv. Mater.* **1993**, 5, 422. (c) Sanchez, C.; Ribot, F. *New. J. Chem.* **1994**, 18, 1007. (d) Schubert, U.; Hüsing, N.; Lorenz, A. *Chem. Mater.* **1995**, 7, 2010. (e) Loy, D. A.; Shea, K. J. *Chem. Rev. (Washington, D.C.)* **1995**, 95, 1431. (f) Judeinstein, P.; Sanchez, C. *J. Mater. Chem.* **1996**, 6, 511.
- (6) (a) Ribot, F.; Banse, F.; Sanchez, C.; Lahcini, M.; Jousseume, B. *J. Sol–Gel Sci. Technol.* **1997**, 8, 529. (b) Angiolini, L.; Caretti, D.; Carlini, C.; De Vito, R.; Niesel, F. T.; Salattelli, E.; Ribot, F.; Sanchez, C. *J. Inorg. Organomet. Polym.* **1998**, 7, in press.

- (7) Mason, J. *Multinuclear NMR*; Plenum Press: New York, 1987; pp 625–629.
- (8) Bax, A.; Davis, D. G. *J. Magn. Reson.* **1985**, 63, 207.
- (9) Yu, C.; Levy, G. *J. Am. Chem. Soc.* **1984**, 106, 6533.
- (10) Bax, A.; Griffey, R. H.; Hawkins, B. L. *J. Magn. Reson.* **1983**, 55, 301.
- (11) (a) Keeler, J.; Clowes, R. T.; Davis, A. L.; Laue, E. D. *Methods Enzymol.* **1994**, 239, 145. (b) Tyburn, J.-M.; Bereton, I. M.; Doddrell, D. M. *J. Magn. Reson.* **1992**, 97, 305. (c) Ruiz-Cabello, J.; Vuister, G. W.; Moonen, C. T. W.; Van Gelderen, P.; Cohen, J. S.; Van Zijl, P. C. M. *J. Magn. Reson.* **1992**, 100, 282. (d) Vuister, G. W.; Boelens, R.; Kaptein, R.; Hurd, R. E.; John B. K.; Van Zijl, P. C. M. *J. Am. Chem. Soc.* **1991**, 113, 9688.
- (12) (a) Kayser, F.; Biesemans, M.; Gielen, M.; Willem, R. *J. Magn. Reson.* **1993**, A102, 249. (b) Martins, J. C.; Kayser, F.; Verheyden, P.; Gielen, M.; Willem, R.; Biesemans, M. *J. Magn. Reson.* **1997**, 124, 128. (c) Kayser, F.; Biesemans, M.; Gielen, M.; Willem, R. *Advanced Applications of NMR to Organometallic Chemistry*; Gielen, M., Willem, R., Wrackmeyer, B., Eds.; Wiley: Chichester, U.K., 1996; Chapter 3, pp 45–86. (d) Willem, R.; Bouhdid, A.; Kayser, F.; Delmotte, A.; Gielen, M.; Martins, J. C.; Biesemans, M.; Tiekink, E. R. T. *Organometallics* **1996**, 15, 1920.
- (13) Reuter, H.; Sebald, A. *Z. Naturforsch.* **1992**, 48B, 195.

recorded to achieve good signal-to-noise ratios. ^{31}P chemical shifts are quoted relative to 85% H_3PO_4 , using solid $NH_4(H_2PO_4)$ as a secondary external reference ($\delta_{iso} = 0.95$ ppm). For both nuclei, at least two experiments, with sufficiently different spinning rates, were run in order to identify the isotropic chemical shifts. The principal components of the ^{119}Sn and ^{31}P shielding tensors were analyzed with WINFIT software¹⁴ using the approach of Herzfeld and Berger.¹⁵ They are reported, following Haeberlen's notation¹⁶ as the isotropic chemical shift ($\delta_{iso} = -\sigma_{iso}$), the anisotropy ($\zeta = \sigma_{33} - \sigma_{iso}$), and the asymmetry ($\eta = |\sigma_{22} - \sigma_{11}|/|\sigma_{33} - \sigma_{iso}|$), σ_{11} , σ_{22} , and σ_{33} being the three components of the shielding tensor expressed in its principal axis system with the following rule: $|\sigma_{33} - \sigma_{iso}| \geq |\sigma_{11} - \sigma_{iso}| \geq |\sigma_{22} - \sigma_{iso}|$.¹⁷ With this writing convention, ζ is a signed value expressed in ppm. The accuracy on δ_{iso} , ζ , and η corresponds to the digital resolution (± 0.5 and ± 0.2 ppm for ^{119}Sn and ^{31}P , respectively), ± 10 ppm, and ± 0.05 , respectively.

Results and Discussion

Synthetic and Chemical Aspects. The chemical constitution of the title compound, mainly the presence of the oxo-hydroxo butyltin cluster, $\{(BuSn)_2O_{14}(OH)_6\}^{2+}$, and of the anionic diphenylphosphinate moieties, is clearly evidenced by its ^{119}Sn , 1H , ^{13}C , and ^{31}P NMR characteristics (vide infra) and chemical analysis. The reaction, in THF, of 2 equiv of diphenylphosphinic acid on $\{(BuSn)_2O_{14}(OH)_6\}(OH)_2$ causes the smooth replacement of the original charge-compensating hydroxyl anions by diphenylphosphinate moieties.



This exchange reaction appears to be quantitative, as observed previously for the analogous preparation of $\{(BuSn)_2O_{14}(OH)_6\}(O_2CH_3)_2$.³

Reaction of $\{(BuSn)_2O_{14}(OH)_6\}(OH)_2$ in THF at room temperature with more than 2 equiv of diphenylphosphinic acid yields a mixture of $\{(BuSn)_2O_{14}(OH)_6\}(O_2PPh_2)_2$ and $\{[BuSn(OH)(O_2PPh_2)]_3O\}(O_2PPh_2)$, this last compound being easily identified by its solution ^{119}Sn NMR signature which consists of a single triplet at -497 ppm ($^2J(^{119}Sn-^{31}P) = 132$ Hz).^{1,18} This trimeric species involves three bridging diphenylphosphinate moieties, covalently bound to tin, and a fourth one which acts as a charge compensating anion.¹⁸ The relative amount of $\{[BuSn(OH)(O_2PPh_2)]_3O\}(O_2PPh_2)$ increases with the excess of Ph_2PO_2H above 2 equiv, and finally $\{[BuSn(OH)(O_2PPh_2)]_3O\}(O_2PPh_2)$ is the only species when 16 equiv of Ph_2PO_2H are used. The quantitative formation of $\{[BuSn(OH)(O_2PPh_2)]_3O\}(O_2PPh_2)$ from the oxo-hydroxo butyltin dication was previously described with $\{(BuSn)_2O_{14}(OH)_6\}Cl_2$ and 16 equiv of Ph_2PO_2H .¹ Yet, with the dichloride cluster, unlike $\{(BuSn)_2O_{14}(OH)_6\}(OH)_2$, the simple exchange of the charge-compensating anions appears impossible. Indeed, when $\{(BuSn)_2O_{14}(OH)_6\}Cl_2$ is reacted in THF with only 2 equiv of Ph_2PO_2H , $\{(BuSn)_2O_{14}(OH)_6\}(O_2PPh_2)_2$ is not obtained, but the reaction yields a mixture of $\{(BuSn)_2O_{14}(OH)_6\}Cl_2$ and $\{[BuSn(OH)(O_2PPh_2)]_3O\}(O_2PPh_2)$, as evidenced by solution ^{119}Sn NMR. The different reactivity of $\{(BuSn)_2O_{14}(OH)_6\}(OH)_2$ and $\{(BuSn)_2O_{14}(OH)_6\}Cl_2$ toward Ph_2PO_2H likely arises from the competition between acido-basic exchange and

Table 1. NMR Data of $\{(BuSn)_2O_{14}(OH)_6\}(O_2PPh_2)_2$ in CD_2Cl_2 at 303 K^{a,b}

coordination state	penta	hexa
1H NMR		
$CH_2(\alpha)$	1.57 [102] ^c	1.09 [127] ^c
$CH_2(\beta)$	1.74 [153] ^c	1.50 [113] ^c
$CH_2(\gamma)$	1.49	1.26
CH_3	0.95	0.84
<i>ortho</i>		7.78
<i>meta + para</i>		7.32
OH		8.23 (broad)
^{13}C NMR		
$CH_2(\alpha)$	21.3 [858/822] ^d	27.0 [1159/1113] ^d
$CH_2(\beta)$	27.0 [49] ^e	28.1 [53] ^e
$CH_2(\gamma)$	26.2 [93] ^e	26.6 [173/166] ^d
CH_3	13.6	13.9
<i>ortho</i>		131.3 {9} ^f
<i>meta</i>		127.9 {12} ^f
<i>para</i>		129.9
<i>ipso</i>		140.3 {130} ^f
^{119}Sn NMR	-283.3 (412 ^g , 158 ^h)	-457.7 (412 ^g , 174 ⁱ)
^{31}P NMR		18.2

^a Chemical shift referencing as in Experimental Section. ^b In solutions of ca. 50 mg of substance per 0.5 mL of solvent. ^c $^nJ(^1H-^{119}Sn)$ coupling constants in Hz, as determined from cross-sections of the 2D $^1H-^{119}Sn$ HMQC spectrum. ^d $^nJ(^{13}C-^{119}Sn)$ and $^nJ(^{13}C-^{117}Sn)$ coupling constants in Hz. ^e Unresolved $^nJ(^{13}C-^{119/117}Sn)$ coupling constants in Hz. ^f $^nJ(^{13}C-^{31}P)$ coupling constants in Hz. ^g Unresolved $^2J(^{119}Sn_p-^{119/117}Sn_h)$ or $^2J(^{119}Sn_h-^{119/117}Sn_p)$ coupling constant in Hz. ^h $^2J(^{119}Sn_p-^{117}Sn_p)$ coupling constant in Hz. ⁱ $^2J(^{119}Sn_h-^{117}Sn_h)$ coupling constant in Hz.

nucleophilic addition to tin. Obviously, Ph_2PO_2H is strong enough an acid to react with OH^- and produce H_2O but not strong enough to react with Cl^- and produce HCl . Therefore, below the charge stoichiometry (2 equiv) and with the dihydroxyl species, the nucleophilic character of diphenylphosphinic acid is not expressed because the diphenylphosphinate moieties that form are trapped as charge-compensating anions. Above the charge stoichiometry with the dihydroxyl species, or with any stoichiometry with the dichloride species, the nucleophilic character of Ph_2PO_2H is not masked by acido-basic exchange, thus leading to the cleavage of the $Sn-O-Sn$ framework of $\{(BuSn)_2O_{14}(OH)_6\}X_2$ and the formation of diphenylphosphinate moieties covalently bound to tin atoms.

Solution NMR Characterization of $\{(BuSn)_2O_{14}(OH)_6\}(O_2PPh_2)_2$. A survey of the NMR data on $\{(BuSn)_2O_{14}(OH)_6\}(O_2PPh_2)_2$ in CD_2Cl_2 solution is given in Table 1. The ^{119}Sn chemical shifts at -283.3 and -457.7 ppm, as well as the associated $^2J(^{119}Sn-O-^{119/117}Sn)$ coupling constant patterns, characterize the pentacoordinated and hexacoordinated tin atoms, respectively, of the closo-cluster.¹⁻⁴ The ^{31}P chemical shift observed at 18.2 ppm is very close to the one (19.4 ppm) reported for the diphenylphosphinate moiety which is not bound to tin and acts as a charge-compensating anion, in $\{[BuSn(OH)(O_2PPh_2)]_3O\}(O_2PPh_2)$.¹ The bridging diphenylphosphinate moieties are reported at 31.0 ppm in this latter compound.¹

1H chemical shifts of the butyl groups bound to the pentacoordinated and hexacoordinated tin atoms, respectively, as well as the corresponding coupling constants were unequivocally assigned by $^1H-^{119}Sn$ HMQC experiments. The ^{13}C chemical shifts were assigned from a $^1H-^{13}C$ HMQC correlation spectrum and $^nJ(^{13}C-^{119}Sn)$ coupling constants for the butyl groups, while the splitting of the aromatic ^{13}C resonances, due to $^{13}C-^{31}P$ coupling, allowed the assignment of the aromatic carbon atoms of the diphenylphosphinate moiety.

(14) Massiot, D.; Thiele, H.; Germanus, A. *Bruker Rep.* **1994**, 140, 43.

(15) Herzfeld, J.; Berger, A. E. *J. Chem. Phys.* **1980**, 73, 6021.

(16) Haeberlen, U. *Adv. Magn. Reson.* **1976** (Suppl. 1).

(17) Harris, R. K.; Lawrence, S. E.; Oh, S. W. *J. Mol. Struct.* **1995**, 347, 309.

(18) Day, R. O.; Holmes, J. M.; Chandrasekhar, V.; Holmes, R. R. *J. Am. Chem. Soc.* **1987**, 109, 940.

All chemical shifts and coupling constants related to the oxo-hydroxy butyltin cluster are very similar to those previously found with different charge-compensating anions (Cl^- , OH^- , AcO^-),^{1–3} except for the μ_2 -OH resonance which was not visible previously, due to extreme broadening. The OH resonance observable in the present system at 8.23 ppm, however, does not show a ^1H – ^{119}Sn HMQC correlation cross-peak at 303 K, which is not surprising given its broadness.

Lowering the temperature to 273 K sharpens the μ_2 -OH resonance, while a second broad OH signal, probably due to some residual water in the sample, becomes visible. Further lowering of the temperature does not induce more sharpening but, on the contrary, further broadening of the μ_2 -OH signal. At 273 K, again no ^1H – ^{119}Sn HMQC correlations were developed for the μ_2 -OH signal. At this temperature a ^1H ROESY correlation spectrum (mixing time 500 ms) reveals exchange cross-peaks between the two types of hydroxylic protons as well as dipolar coupling cross-peaks between the μ_2 -OH protons at 8.29 ppm and the $\text{CH}_2(\alpha)$ and $\text{CH}_2(\beta)$ protons of the butyl groups bound to the hexacoordinated tin atoms, thus indicating that the latter hydroxylic protons are indeed located in the proximity of the hexacoordinated tin atoms.^{1,2}

Other proximity evidences were found in ^{31}P – ^1H heteronuclear Overhauser spectroscopy (HOESY) spectra (mixing times 100, 500, and 1000 ms). Cross-peaks were detected, as expected, between the ^{31}P nucleus of the charge-compensating Ph_2PO_2^- and the ortho protons of its aromatic rings but also, and more importantly, between the ^{31}P nucleus and the $\text{CH}_2(\alpha)$ and $\text{CH}_2(\beta)$ protons of the butyl groups on the hexacoordinated tin atoms as well as the μ_2 -OH protons. If it is assumed that the distance between the phosphorus atom and the ortho protons of the diphenylphosphinate anions is known and constant, because of the well-defined anion geometry, it can be taken as an internal reference distance in the estimation of the distance between the other protons and the phosphorus atom using the equation $r_i = r_{\text{ref}} (k_{\text{ref}}/k_i)^{1/6}$.¹⁹ In this equation, r_i represents the interatomic distance of interest and r_{ref} the reference distance, while k_i and k_{ref} are the slopes of the respective buildup straight lines, in the initial rate approximation, associated with the cross-peaks correlating the pairs of nuclei under consideration. However, because ^{31}P – ^1H HOESY experiments are very time consuming, no complete buildup was performed and the volumes of the cross-peaks were used in the calculation instead of the slopes of the buildup straight line. Spin diffusion was ruled out by the observation that the relative intensities of the OH, the $\text{CH}_2(\alpha)$, and the $\text{CH}_2(\beta)$ cross-peaks with the ^{31}P nucleus remain identical within experimental error upon mixing time increase. Taking as reference distance between the phosphorus atom and the ortho protons the value of 2.93 ± 0.05 Å, calculated on the anionic diphenylphosphinate moiety of $\{[\text{BuSn}(\text{OH})(\text{O}_2\text{PPh}_2)_3\text{O}](\text{O}_2\text{PPh}_2)_2\}$,²⁰ the distances between the phosphorus and the other protons of $\{(\text{BuSn})_{12}\text{O}_{14}(\text{OH})_6\}(\text{O}_2\text{PPh}_2)_2$ were estimated at 3.0, 3.3, and 3.6 Å for the μ_2 -OH, the $\text{CH}_2(\alpha)$ and $\text{CH}_2(\beta)$ groups, respectively. These results clearly show that, in CD_2Cl_2 , the anionic diphenylphosphinates are close to the “poles” of $\{(\text{BuSn})_{12}\text{O}_{14}(\text{OH})_6\}^{2+}$, as expected from an electrostatic interaction in low dielectric constant media.

It is very interesting to note that the structure of the tin–oxygen framework of $\{[\text{BuSn}(\text{OH})(\text{O}_2\text{PPh}_2)_3\text{O}]\}^+$ is extremely close to the one encountered at each “cage pole” of $\{(\text{BuSn})_{12}\text{O}_{14}(\text{OH})_6\}^{2+}$ (see Figures 1 and 2).^{1,2,18} Even though

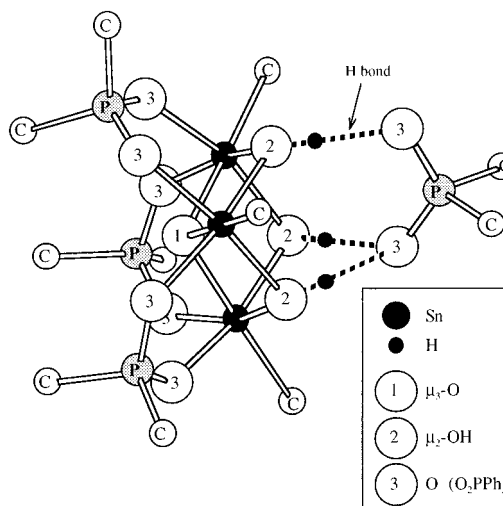


Figure 2. Molecular drawing of $\{[\text{BuSn}(\text{OH})(\text{O}_2\text{PPh}_2)_3\text{O}](\text{O}_2\text{PPh}_2)\}^{18}$. For clarity, only the α -carbon of each butyl chain and the *ipso*-carbon of each phenyl ring are shown. The positions of the hydrogen atoms of the three μ_2 -OH groups have been computed.²⁰

the oxygen atoms of the bridging diphenylphosphinate moieties in $\{[\text{BuSn}(\text{OH})(\text{O}_2\text{PPh}_2)_3\text{O}]\}^+$ become μ_3 -O atoms connecting a six-coordinate tin atom to two five-coordinate tin atoms in $\{(\text{BuSn})_{12}\text{O}_{14}(\text{OH})_6\}^{2+}$, all the Sn–O, Sn–C, and Sn–Sn distances remain, pairwise, equal within 0.04 Å, when both structures are compared. Actually, the main structural difference lies in the angles formed by the α -carbon of the butyl chains, the tin atoms and the μ_3 -O atom connecting the three six-coordinate tin atoms. They are close to 178° in $\{[\text{BuSn}(\text{OH})(\text{O}_2\text{PPh}_2)_3\text{O}]\}^+$, while they are close to 170° in $\{(\text{BuSn})_{12}\text{O}_{14}(\text{OH})_6\}^{2+}$.^{1,2,18} This quite small difference likely arises from larger constraints in $\{(\text{BuSn})_{12}\text{O}_{14}(\text{OH})_6\}^{2+}$, which exhibits a close Sn–O–Sn framework.^{1,2}

In crystalline $\{[\text{BuSn}(\text{OH})(\text{O}_2\text{PPh}_2)_3\text{O}](\text{O}_2\text{PPh}_2)\}$, the three distances between the phosphorus atom of the anionic diphenylphosphinate and the hydrogen atoms of the bridging hydroxy groups are 2.59, 2.83, and 2.85 Å.^{18,20} These values, though they are shorter, are quite similar to the one of 3.0 Å determined by the present ^{31}P – ^1H HOESY experiment. Therefore, it appears that when $\{(\text{BuSn})_{12}\text{O}_{14}(\text{OH})_6\}(\text{O}_2\text{PPh}_2)_2$ is dissolved in CD_2Cl_2 , the anionic diphenylphosphinate moieties are almost as close to the bridging hydroxy groups located at the “cage poles” (Figure 1) as they are in crystalline $\{[\text{BuSn}(\text{OH})(\text{O}_2\text{PPh}_2)_3\text{O}](\text{O}_2\text{PPh}_2)\}$ (Figure 2); accordingly, the same type of hydrogen bonding is likely involved. Actually, the geometry observed in the crystalline structure of $\{[\text{BuSn}(\text{OH})(\text{O}_2\text{PPh}_2)_3\text{O}](\text{O}_2\text{PPh}_2)\}$ (Figure 2) probably represents the closest

(20) The positions of the hydrogen atoms, which were not reported in the X-ray structure of $\{[\text{BuSn}(\text{OH})(\text{O}_2\text{PPh}_2)_3\text{O}](\text{O}_2\text{PPh}_2)\}$,¹⁸ were computed as follows. For the phenyl and the butyl groups, CRYSTALS software²¹ was used with a C–H distance set to 1.08 Å.²⁵ In this procedure, the hybridization of the carbon and the conformation of the butyl chain are taken into account. The four P–H_{ortho} distances found for the anionic diphenylphosphinate are 2.887, 2.921, 2.944, and 2.981 Å, resulting in a mean value of 2.93 Å with a deviation of about 0.05 Å. For comparison, the mean P–H_{ortho} distance for the three bridging diphenylphosphinate groups is 2.89 Å, slightly shorter (with a minimum of 2.824 Å and a maximum of 2.946 Å). For the μ_2 -OH, which are reported to exchange hydrogen bonds with the charge-compensating diphenylphosphinate,¹⁸ the hydrogen atoms were placed on the line linking a given bridging oxygen and the closest oxygen of the anionic diphenylphosphinate, with a proton–bridging oxygen distance of 1.00 Å.

(21) Watkin, D. J.; Prout, C. K.; Carruthers, J. R.; Betteridge, P. W. *CRYSTALS*; Chemical Crystallography Laboratory, University of Oxford: Oxford, U.K., 1996; Issue 10.

(19) Neuhaus, D.; Williamson, M. P. *The Nuclear Overhauser Effect in Structural and Conformational Analysis*; VCH: New York, 1989; pp 104–109.

Table 2. NMR Data of $\{(BuSn)_2O_{14}(OH)_6\}(O_2PPh_2)_2$ in $CD_2Cl_2/DMSO-d_6$ at 308 K^{a,b}

coordination state	penta	hexa
¹ H NMR		
CH ₂ (α)	1.35–1.50 ^d	0.96 [128] ^c
CH ₂ (β)	1.68 [~132] ^e	1.46 [101] ^c
CH ₂ (γ)	1.35–1.50 ^d	1.18
CH ₃	0.87	0.78
ortho		7.66
meta + para		7.26
OH		7.96 and 3.16
¹¹⁹ Sn NMR	–306.9 (broad, Δν _{1/2} ~ 700 Hz)	–466.7 (406 ^f , 204 ^g)
³¹ P NMR		15.0

^a Chemical shifts referencing as in Experimental Section. ^b In solutions of ca. 50 mg of substance per 0.5 mL of solvent. ^c $^nJ(^1H-^{119}Sn)$ coupling constants in Hz, as determined from cross-sections of 2D $^1H-^{119}Sn$ HMQC spectra. ^d Not defined exactly due to overlap and lack of cross-peaks in $^1H-^{119}Sn$ HMQC. ^e Unresolved $^3J(^1H-^{119/117}Sn)$ as determined from 1D 1H NMR spectrum. ^f $^2J(^{119}Sn_p-^{119/117}Sn_h)$ or $^2J(^{119}Sn_h-^{119/117}Sn_p)$ coupling constant in Hz. ^g $^2J(^{119}Sn_h-^{117}Sn_h)$ coupling constant in Hz.

possible approach of the diphenylphosphinate anion. Comparison of the distances, determined by solution NMR on $\{(BuSn)_2O_{14}(OH)_6\}(O_2PPh_2)_2$, between the phosphorus and the hydrogen atoms of the CH₂(α) and CH₂(β) groups (3.2 and 3.5 Å, respectively), with the corresponding ones calculated from the structure of $\{[BuSn(OH)(O_2PPh_2)]_3O\}(O_2PPh_2)$ ^{18,20} is less relevant as they strongly depend on the conformation of the butyl chains, which is “frozen” in the crystalline state. Indeed, the various conformations spread these distances quite a lot, as evidenced by their ranges from 5.03 to 6.51 Å and from 3.10 to 6.69 Å, for CH₂(α) and CH₂(β) groups, respectively, in crystalline $\{[BuSn(OH)(O_2PPh_2)]_3O\}(O_2PPh_2)$. However, the shorter distance (3.10 Å) which is found for a CH₂(β) group with a quite favorable conformation is compatible with the distances found by NMR.

As anisochrony is not visible at neither the six-coordinate ¹¹⁹Sn resonance nor the μ₂-OH proton resonance, even at low temperature, it should be concluded that, in solution, the Ph₂PO₂[–] anion cannot be “locked” on the three bridging hydroxy groups, at least on the NMR time scale, as it is in the structure of $\{[BuSn(OH)(O_2PPh_2)]_3O\}(O_2PPh_2)$. Both Ph₂PO₂[–] anions of $\{(BuSn)_2O_{14}(OH)_6\}(O_2PPh_2)_2$ probably undergo, in solution, a spinning motion about their own axis (C₂ symmetry), similar to a merry-go-round, by which their two oxygen atoms are oriented, on average during equal times, toward the three bridging hydroxy groups. This motion suggests that the phosphorus atoms remain essentially immobile and located onto or close to the C₃ axis of the cluster. This interpretation explains the uniqueness of the six-coordinate ¹¹⁹Sn and the μ₂-OH proton resonances, as well as those of the phenyl rings of the anions.

As it was anticipated that a solvent with a higher dielectric constant could promote ionic dissociation, experiments were also run in a mixture of CD₂Cl₂/DMSO-*d*₆ (1/1 vol). Such a solvent mixture was chosen, because, surprisingly, $\{(BuSn)_2O_{14}(OH)_6\}(O_2PPh_2)_2$ appeared insoluble in pure DMSO-*d*₆ (ε = 46.7). This observation, in its own, is not supporting significant ionic dissociation, if any. Table 2 summarizes the NMR parameters obtained in this solvent mixture at 308 K. A slightly higher temperature was used because of this restricted solubility.

A shift of about 10 ppm to low frequency is observed for the hexacoordinated ¹¹⁹Sn resonance. That of the pentacoor-

inated tin atoms undergoes an even more pronounced shift to low frequency of about 25 ppm and, simultaneously, a substantial broadening. Due to this broadening, only the protons associated with the hexacoordinated tin atoms are edited in a $^1H-^{119}Sn$ HMQC correlation experiment. By contrast, and unlike spectra from pure CD₂Cl₂ solutions, very sharp OH resonances are now observed at 7.96 and 3.16 ppm. One of them (7.96 ppm) gives a well-marked $^1H-^{119}Sn$ HMQC correlation cross-peak, thus evidencing the existence of a $^2J(^1H-^{119}Sn)$ coupling between the μ₂-OH protons and the hexacoordinated tin atoms. The other hydroxylic proton is assigned to a small amount of water present in the sample.

As for pure CD₂Cl₂, exchange cross-peaks between the two types of hydroxylic protons are again observed (at 308 instead of 273 K) in a 1H ROESY spectrum as are dipolar coupling cross-peaks between the μ₂-OH and the CH₂(α) as well as the CH₂(β) protons of the butyl groups on the hexacoordinated tin atoms, again confirming the spatial proximity of these μ₂-OH protons and these hexacoordinated tin atoms. ³¹P- 1H HOESY experiments still reveal a correlation between the phosphorus and the μ₂-OH but, importantly, no longer with the CH₂(α) and CH₂(β) protons of the butyl groups. Using the same internal reference, *d*(P-H_{ortho}), the μ₂-OH–P distance was estimated at 3.5 Å in the present case of CD₂Cl₂/DMSO-*d*₆, instead of 3.0 Å in pure CD₂Cl₂.

These results suggest a looser, but still present, electrostatic interaction between the Ph₂PO₂[–] anions and the cluster. The Ph₂PO₂[–] anions are still in the vicinity of the cluster “cage poles”, yet they appear further remote from the μ₂-OH, as compared to pure CD₂Cl₂. Moreover, the higher sharpness of the OH resonances as well as the higher observation temperature, as compared to pure CD₂Cl₂ solutions, indicates a lower tendency of the protons to be split off and to exchange with water protons, suggesting that the hydroxylic μ₂-OH protons are less involved in a strong hydrogen bridge pattern and, accordingly, more strongly bound to the μ₂-OH oxygens. Therefore, the larger separation of the anions, via their weaker hydrogen bonds with the bridging hydroxy groups, causes an increase in the shielding of the hexacoordinated tin atoms, as evidenced by the 10 ppm high-field shift of their ¹¹⁹Sn resonance. Correlatively, the increase of the anion–cluster separation explains that the distances between the phosphorus and the CH₂(α) and CH₂(β) protons are too long to be detected by ³¹P- 1H HOESY experiments (1/*r*⁶ contribution). Of course, the persistence of a single ¹¹⁹Sn and 1H resonance for six-coordinate tin atoms and for the μ₂-OH moiety indicates again that the Ph₂PO₂[–] anions are still experiencing the same kind of motion which averages the geometrical features of their now weak interaction with the clusters’ “cage poles”.

The change in the strength of the interaction between the anions and the cluster “poles” is most likely not responsible for the 25 ppm low-frequency shift of the pentacoordinated tin atoms which are too remote anyway. Indirect evidences are the small variations, within 5 ppm, of the pentacoordinated ¹¹⁹Sn resonance, while the hexacoordinated ¹¹⁹Sn resonance can be shifted by up to 15 ppm, when the counteranions of $\{(BuSn)_2O_{14}(OH)_6\}^{2+}$ are varied (Cl[–], OH[–], OAc[–], CH₃C₆H₄SO₃[–]).^{1–4} Thus, the present 25 ppm low-frequency shift, as well as the line broadening, is solvent related and probably due to an interaction between the pentacoordinated tin atoms (Lewis acid) and the oxygen atom of the DMSO molecules (Lewis base). Addition of a weak Sn–O contact onto a five-coordinate tin should indeed result in the observed increased shielding.

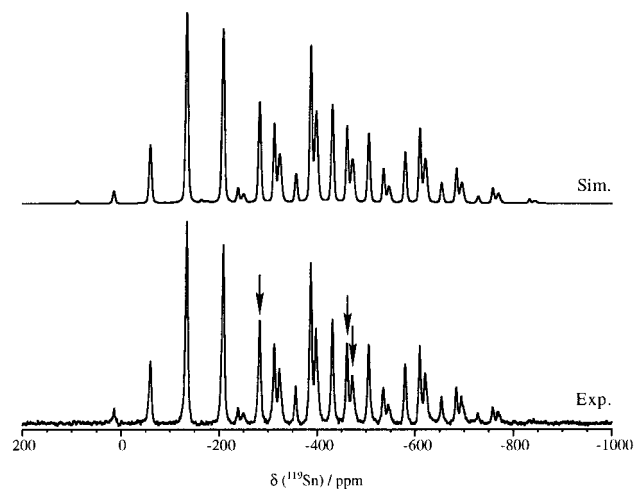


Figure 3. ^{119}Sn MAS NMR spectrum of $\{(\text{BuSn})_{12}\text{O}_{14}(\text{OH})_6\}(\text{O}_2\text{PPh}_2)_2$. Isotropic resonances are shown with arrows ($\nu_{\text{MAS}} = 8300$ Hz).

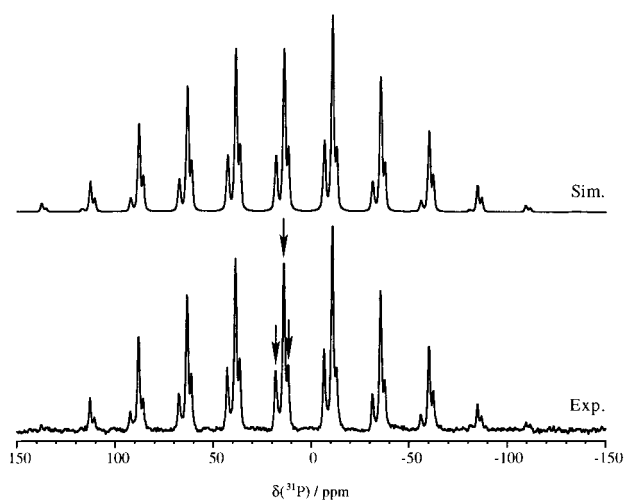


Figure 4. $^{31}\text{P}-\{^1\text{H}\}$ MAS NMR spectrum of $\{(\text{BuSn})_{12}\text{O}_{14}(\text{OH})_6\}(\text{O}_2\text{PPh}_2)_2$. Isotropic resonances are shown with arrows ($\nu_{\text{MAS}} = 3000$ Hz).

Table 3. Solid State ^{119}Sn NMR Data for $\{(\text{BuSn})_{12}\text{O}_{14}(\text{OH})_6\}(\text{O}_2\text{PPh}_2)_2^a$

site	δ_{iso} ppm	ζ ppm	η	σ_{11} ppm	σ_{22} ppm	σ_{33} ppm	area %	CN
1	-282.7	386.5	0.20	50.8	128.1	669.2	50	5
2	-461.3	304.7	0.25	270.9	347.0	766.0	27	6
3	-472.4	312.2	0.15	292.9	339.7	784.6	23	6

^a $\delta_{\text{iso}} = -\sigma_{\text{iso}} = -(\sigma_{11} + \sigma_{22} + \sigma_{33})/3$; $\zeta = \sigma_{33} - \sigma_{\text{iso}}$; $\eta = |\sigma_{22} - \sigma_{11}|/|\sigma_{33} - \sigma_{\text{iso}}|$. σ_{11} , σ_{22} , and σ_{33} are the principal components of the ^{119}Sn shielding tensor, ordered with the following rule: $|\sigma_{33} - \sigma_{\text{iso}}| \geq |\sigma_{11} - \sigma_{\text{iso}}| \geq |\sigma_{22} - \sigma_{\text{iso}}|$.¹⁷

Solid-State NMR Characterization of $\{(\text{BuSn})_{12}\text{O}_{14}(\text{OH})_6\}(\text{O}_2\text{PPh}_2)_2$. The solid state ^{119}Sn and ^{31}P MAS NMR spectra of $\{(\text{BuSn})_{12}\text{O}_{14}(\text{OH})_6\}(\text{O}_2\text{PPh}_2)_2$ are presented, with their simulation, in Figures 3 and 4, respectively. The data extracted from the simulations are gathered in Tables 3 and 4, respectively. The ^{31}P NMR data for $\text{Ph}_2\text{PO}_2\text{H}$ are also reported in Table 4 for comparison.

Three ^{31}P sites are evidenced, the major one being at 14.0 ppm. The observed isotropic ^{31}P chemical shifts are close to the solution values but are fairly different from the isotropic chemical shift of 28.5 ppm for solid $\text{Ph}_2\text{PO}_2\text{H}$. Therefore, the three species observed by ^{31}P NMR are all anionic diphenylphosphinates interacting with $\{(\text{BuSn})_{12}\text{O}_{14}(\text{OH})_6\}^{2+}$. This

Table 4. Solid State ^{31}P NMR Data for $\{(\text{BuSn})_{12}\text{O}_{14}(\text{OH})_6\}(\text{O}_2\text{PPh}_2)_2$ and $\text{Ph}_2\text{PO}_2\text{H}^a$

site	δ_{iso} ppm	ζ ppm	η	σ_{11} ppm	σ_{22} ppm	σ_{33} ppm	area %
a	11.8	106.2	0.95	94.4	-14.5	-115.3	21
b	14.0	101.2	0.90	82.2	-8.9	-115.2	62
c	18.1	79.0	0.85	55.0	-12.1	-97.1	17
$\text{Ph}_2\text{PO}_2\text{H}$	28.5	-91.5	0.80	-110.8	-37.7	62.9	100

^a See legend to Table 3.

indicates three well-defined interaction geometries between the diphenylphosphinate anions and the macrocation rather than a distribution of geometries, as might be expected for an amorphous solid. However, the solid state ^{31}P NMR being very sensitive, the three types of diphenylphosphinate anions might only reflect small changes in the P–X bonds length or X–P–Y angles (X = O or C and Y = O or C).²² As very little literature is available on the ^{31}P shielding tensors of phosphinic acids or their derivatives,²³ discussion of the principal components reported in Table 4 is not relevant, yet it can only be noted that the asymmetries (η) are close to unity. Actually, for phosphorus atoms immobile on the NMR time scale and which exhibit at highest a C_{2v} symmetry, asymmetries different from zero (nonaxial symmetries) could have just been predicted. Inferring or comparing the local structures around the phosphorus atoms from their NMR characteristics is also difficult at the moment, yet the site labeled c appears to be the most different according to the principal components of its shielding tensor.

Three ^{119}Sn sites, with their pattern of spinning sidebands, are also clearly observed on the spectrum. Assignment of their coordination numbers (CN) is straightforward from the solution study and literature.^{2,3,13} One site, $\delta_{\text{iso}} = -282.7$ ppm, corresponds to five-coordinate tin atoms and accounts for half of the nuclei, as expected for the structure of $\{(\text{BuSn})_{12}\text{O}_{14}(\text{OH})_6\}^{2+}$. Its isotropic chemical shift agrees very well with the value obtained in CD_2Cl_2 solution, a solvent exhibiting no particular interaction. The two others, $\delta_{\text{iso}} = -461.3$ and -472.4 ppm, are both assigned to six-coordinate tin atoms, and each accounts for approximately 25% of the ^{119}Sn nuclei. Their area weighted average of -466.4 ppm matches perfectly well the high-field resonance of $\{(\text{BuSn})_{12}\text{O}_{14}(\text{OH})_6\}(\text{O}_2\text{PPh}_2)_2$ in $\text{CD}_2\text{Cl}_2/\text{DMSO}-d_6$. According to the solution study, the diphenylphosphinate anions would be, on average over the different interactions evidenced by ^{31}P MAS NMR, more distant from the “cage poles” than they are in CD_2Cl_2 . Yet, a 10 ppm shift between solution and solid state can have other origins. The ^{119}Sn resonance duplication for the hexacoordinated tin atoms with respect to the solution state clearly evidences a decrease in the apparent symmetry of the “cage poles”, likely toward C_{2h} . This phenomenon was previously observed for other derivatives of $\{(\text{BuSn})_{12}\text{O}_{14}(\text{OH})_6\}^{2+}$.^{2,3} However, the almost equal population of these two sites is puzzling, since the lower symmetry of the phosphinate anions should provide either three equally populated sites or two sites in a population ratio of 2:1. These equal populations apparently result from fortuitous overlappings. Indeed, three types of diphenylphosphinate anions were evidenced by ^{31}P MAS NMR. The more abundant (60%) type would split the six-coordinate tin atoms of the “cage poles” in two sites A and B with relative areas of 2 and 1, respectively, while the two other types of diphenylphosphinate anions (40%) would give the same splitting, A and B, but with reverse relative

(22) Un, S.; Klein, M. P. *J. Am. Chem. Soc.* **1989**, *111*, 5119.

(23) Harris, R. K.; Merwin, L. H.; Hägele, G. *J. Chem. Soc., Faraday Trans 1* **1989**, *85*, 1409.

areas of 1 and 2, respectively. With these overlappings, the sites A and B would represent 27 and 23% of the total area, respectively, matching perfectly the experimental results. This proposal is of course not a univocal explanation.

The principal components of the ^{119}Sn shielding tensors are close to those previously reported for $\{(\text{BuSn})_{12}\text{O}_{14}(\text{OH})_6\}(\text{OH})_2\cdot(\text{iPrOH})_4$ and $\{(\text{BuSn})_{12}\text{O}_{14}(\text{OH})_6\}(\text{O}_2\text{CCH}_3)_2$.^{2,3} As expected from their local geometries (see Figure 1), the five-coordinate tin atoms exhibit larger anisotropies (ζ) compared to six-coordinate ones.¹³ The asymmetries (η) are close to zero, indicating near-axial symmetries what would be the case in ideal square pyramidal (CSnO_4) or pseudo-octahedral (CSnO_5) environments.²⁴

Finally, it appears difficult to conclude whether the geometry of the interaction evidenced in the structure of $\{[\text{BuSn}(\text{OH})(\text{O}_2\text{PPh}_2)]_3\text{O}\}(\text{O}_2\text{PPh}_2)_2$ ¹⁸ (see Figure 2) and likely present when $\{(\text{BuSn})_{12}\text{O}_{14}(\text{OH})_6\}(\text{O}_2\text{PPh}_2)_2$ is dissolved in CD_2Cl_2 is also found in the solid. Actually, the diphenylphosphinate anions might also bridge two macrocations, as do the charge-compensating anions in crystallized $\{(\text{BuSn})_{12}\text{O}_{14}(\text{OH})_6\}\text{Cl}_2\cdot(\text{H}_2\text{O})_2$ and $\{(\text{BuSn})_{12}\text{O}_{14}(\text{OH})_6\}(\text{OH})_2\cdot(\text{iPrOH})_4$.^{1,2}

Conclusion

The present multinuclear NMR approach has clearly shown that, in low or medium dielectric constant solvent, the charge-

compensating diphenylphosphinate anions, even though involved in a spinning motion, remain in the vicinity of the "cage poles" of $\{(\text{BuSn})_{12}\text{O}_{14}(\text{OH})_6\}^{2+}$. The geometry of the interaction is difficult to infer precisely, but it is likely similar to the one observed in crystalline $\{[\text{BuSn}(\text{OH})(\text{O}_2\text{PPh}_2)]_3\text{O}\}(\text{O}_2\text{PPh}_2)_2$ ¹⁸ and involves electrostatic attraction as well as multiple hydrogen bonds. The persistence of strong macrocation-anion contacts in solution can probably be extrapolated to $\{(\text{BuSn})_{12}\text{O}_{14}(\text{OH})_6\}^{2+}$ with other counteranions such as OH^- , Cl^- , CH_3CO_2^- , or $p\text{-CH}_3\text{C}_6\text{H}_4\text{SO}_3^-$, thus explaining the influence of the anions on the ^{119}Sn chemical shift of the six-coordinate tin atoms.¹⁻⁴

The persistence in solution of these interactions allows their use to assemble or functionalize $\{(\text{BuSn})_{12}\text{O}_{14}(\text{OH})_6\}^{2+}$ clusters and prepare hybrid organic-inorganic polymers.^{3,4,6}

Acknowledgment. Partial funding of this research by Contract ERBCHRX-CT94-0610 of the Human Capital & Mobility (HCM) Programme of the European Union is acknowledged (C.S., R.W.). The financial support of the Belgian National Science Foundation (FKFO, Grant NR 2.0094.94) and of the Belgian "Nationale Loterij" (Grant NR 9.0006.93) is also acknowledged (R.W., M.B.). R.W. and M.B. thank Mrs. I. Verbruggen for technical assistance. J.C.M. is a postdoctoral researcher of the Flemish "Fonds voor Wetenschappelijk Onderzoek Vlaanderen". F.R. and C.S. thank Ms. N. Steunou for her help with CRYSTALS software.

IC971189R

(24) Klaus, E.; Sebal, A. *Magn. Reson. Chem.* **1994**, *32*, 679-690.

(25) March, J. R. *Advanced Organic Chemistry*; J. Wiley & Sons: New York, 1992; p 21.